

Polymer Chemistry

Accepted Manuscript



This is an *Accepted Manuscript*, which has been through the Royal Society of Chemistry peer review process and has been accepted for publication.

Accepted Manuscripts are published online shortly after acceptance, before technical editing, formatting and proof reading. Using this free service, authors can make their results available to the community, in citable form, before we publish the edited article. We will replace this *Accepted Manuscript* with the edited and formatted *Advance Article* as soon as it is available.

You can find more information about *Accepted Manuscripts* in the [Information for Authors](#).

Please note that technical editing may introduce minor changes to the text and/or graphics, which may alter content. The journal's standard [Terms & Conditions](#) and the [Ethical guidelines](#) still apply. In no event shall the Royal Society of Chemistry be held responsible for any errors or omissions in this *Accepted Manuscript* or any consequences arising from the use of any information it contains.

Novel sulfonated poly(arylene ether sulfone) containing hydroxyl groups for enhanced proton exchange membrane properties

Cite this: DOI: 10.1039/x0xx00000x

Received 00th January 2012,
Accepted 00th January 2012

DOI: 10.1039/x0xx00000x

www.rsc.org/

Yeonhye Kwon^{a,b}, So Young Lee^a, Sukjae Hong^a, Jong Hyun Jang^a, Dirk Henkensmeier^a, Sung Jong Yoo^a, Hyoung-Juhn Kim^{*a}, Sung-Hyun Kim^{**b}

We here report a new sulfonated poly(arylene ether sulfone) modified with hydroxyl side groups for a proton exchange membrane fuel cell (PEMFC). The polymer was synthesized via 4-step reaction including direct copolymerization, sulfochlorination, demethylation, and hydrolysis. By adding the hydroxyl group into the polymer backbone, strong intermolecular hydrogen bonds could be generated between polymer chains. The hydroxyl sulfonated polymer demonstrated high proton conductivities under a variety of temperatures and relative humidities due to its enhanced phase-separated morphology. Moreover, it showed improved fuel cell performance compared to the non-hydroxylated analog with the same sulfonation degree. The introduction of hydroxyl groups to the sulfonated poly(arylene ether sulfone) provides a potential candidate for an improved PEMFC membrane.

Introduction

Owing to the increasing need for clean energy conversion systems, proton exchange membrane fuel cells (PEMFCs) are being developed as a promising alternative to the use of fossil fuels as energy generating systems.¹⁻⁹ As one of the main components of PEMFCs, proton exchange membranes (PEMs) that are cheaper and are synthesized via a more simplified procedure are essential for advancing this technology.¹⁰⁻¹² The most widely used PEM is currently perfluorinated sulfonic acid (PFSA) membranes which show superior properties including high proton conductivity and durability in the temperature range of 20–80 °C.¹³⁻¹⁵ However, this material has several drawbacks such as high cost and a complex synthetic protocol.^{16,17}

To date, many efforts have been made in order to enhance the properties of PEMs containing hydrocarbon-based aromatic backbones including sulfonated derivatives of poly(arylene ether sulfone)s.¹⁸⁻²² What is a significant problem of hydrocarbon-based PEMs has been recognized as the inferior dimensional stability caused by high water uptake of membrane

as a degree of sulfonation increases.^{23, 24} This is because the high sulfonation degree results in the high connectivity of hydrophilic phase and high solubility in water in spite of its enhanced proton conductivity.^{25,26} Therefore, several approaches to improve the proton conductivity of a membrane without influencing the insolubility in water have been examined, for example, fabricating composite membranes^{27,28}, introducing acidic functionalities to polymer backbones²⁹⁻³¹, and changing the position of sulfonic acid groups.³²⁻³⁴ Composite membranes, composed of an inorganic substrate and a polymer electrolyte which fills the pores of the substrate, showed improvement in their water retention properties and thermal properties. However, due to the different natures of organic and inorganic materials, they were found to have mechanically unstable property caused by their low compatibility and uneven distribution of inorganic contents.³⁵

In our effort to overcome these drawbacks, we have adopted an approach introducing a novel functionality into polymer backbone which has possibility to enhance the proton conductivity as well as the water insolubility. McKeen et al., reported that a sulfonic acid-functionalized zeolite possessing dangling hydroxyl groups could be applied as an oxide additive in a PEM, and demonstrated a proton conductivity of 68 mS/cm when fully humidified at room temperature.³⁶ Inspired by this earlier research, we suggest that the intermolecular force induced by hydroxyl group could be helpful to enhance the fuel cell performance in a given membrane system.

In this study, we introduced a hydroxyl group into a sulfonated poly(arylene ether sulfone). Such a functional

^a Fuel Cell Research Center, Korea Institute of Science and Technology (KIST), 5, Hwarang-ro 14-gil, Seongbuk-gu, Seoul 136-791, Republic of Korea. E-mail: hjkim25@kist.re.kr

^b Department of Chemical and Biological Engineering, Korea University, 145, Anam-ro, Seongbuk-gu, Seoul 136-701, Republic of Korea. E-mail: kimsh@korea.ac.kr

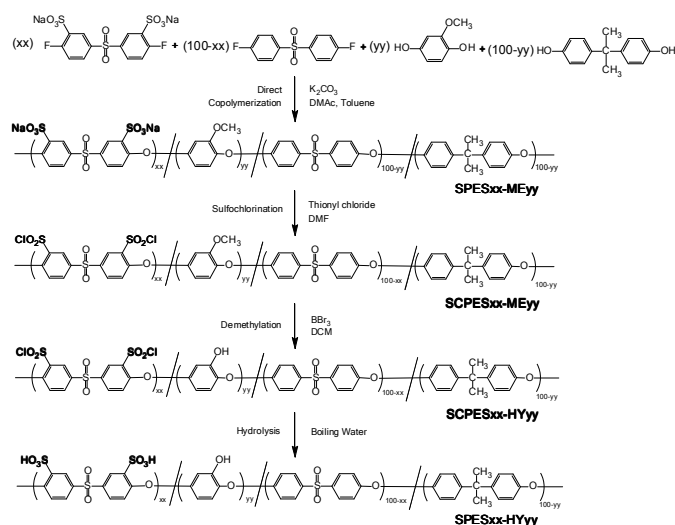
† Electronic Supplementary Information (ESI) available: Polarization curves of SPAES30-HY00 and SPAES30-HY30, excluding the effect of ohmic resistance. See DOI: 10.1039/b000000x/

moiety should provide the high possibility for hydrogen bonding with other hydroxyl groups, sulfonated groups, and water; therefore, it should improve proton conductivity as well as the mechanical properties of the membrane. Furthermore, the introduction of a hydroxyl group to the polymer would not increase the solubility in water as much as a sulfonated group would.

Results and discussion

Synthesis of sulfonated poly(arylene ether sulfone) containing hydroxyl groups

Poly(arylene ether sulfone) modified with hydroxyl groups was synthesized via the four-step reaction shown in **Scheme 1**. The sulfonated poly(arylene ether sulfone) (SPES_{xx}-ME_{yy}) was synthesized through a polycondensation reaction using *N*-methyl-2-pyrrolidone (NMP) as solvent. To synthesize the hydroxyl sulfonated polymer (SPES_{xx}-HY_{yy}), SPES_{xx}-ME_{yy} needed to be dissolved in dichloromethane (DCM) for the demethylation process to occur. Unfortunately, owing to the presence of the sulfonated group, the SPES_{xx}-ME_{yy} was found to be insoluble in DCM. Thus, a sulfochlorination process using thionyl chloride was carried out in order to obtain a chlorosulfonated polymer (SCPES_{xx}-ME_{yy}) that was soluble in DCM. After demethylation and hydrolysis, the final product, sulfonated poly(arylene ether sulfone) with hydroxyl groups, SPES_{xx}-HY_{yy}, was formed.



Scheme 1 Synthesis procedures of copolymers (SPES_{xx}-ME_{yy}, SCPES_{xx}-ME_{yy}, SCPES_{xx}-HY_{yy}, and SPES_{xx}-HY_{yy}).

We fixed the molar ratio of monomers to synthesize SPES30-HY30 ($xx = 30$: bis(4-fluoro-3-sulfophenyl) sulfone disodium salt/bis(4-fluorophenyl) sulfone = 30/70, and $yy = 30$: 2-methoxyhydroquinone/bisphenol A = 30/70). As shown in **Fig. 1**, the degree of sulfonation (DS = 30%) and molar ratio of methoxy groups (30%) could be determined using ^1H NMR analysis. As represented in **Fig. 1a**, the hydrogen peak corresponding to the methoxy group at around 3.70 ppm was

split into two, which was attributed to the effect of a sulfonic acid group near the randomly site-arranged methoxy group in the hydroquinone. Furthermore, this phenomenon was found in SPES30-ME100, which contained 100% methoxyhydroquinone instead of bisphenol-A (**Fig. 2**). After the demethylation process, the total disappearance of the two proton signals corresponding to hydrogens in the methoxy group indicated that the demethylation of the polymer was complete, and that the hydroxyl group was successfully introduced (**Fig. 1b**). The FT-IR spectra of the three fabricated membranes, SPES30-ME30, SCPES30-ME30, and SPES30-HY30, are shown in **Fig. 3**. The typical band for a sulfonyl chloride is in the region 1385–1360 cm^{-1} .³⁸ For the spectrum of SCPES30-ME30, this band was found at around 1370 cm^{-1} , and was not visible in the spectrum for SPES30-ME30, which demonstrates that the sulfonyl chloride group was successfully introduced into the polymer. In addition, the band disappeared after hydrolysis of the membrane, confirming that the sulfonyl chloride groups were converted into sulfonic acid groups.

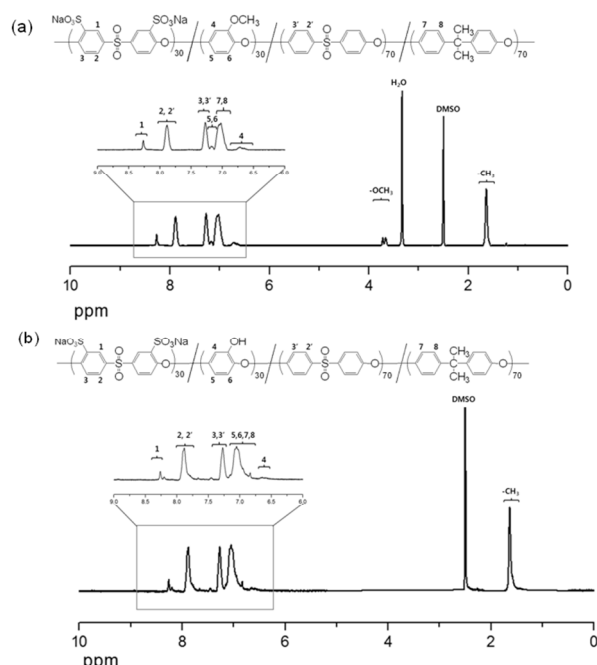


Fig. 1 ^1H NMR spectra of (a) SPES30-ME30 ($-\text{OCH}_3$) and (b) SPES30-HY30 ($-\text{OH}$).

Polymer characteristics

In order to evaluate the effect of hydroxyl groups in the membrane, the sulfonated poly(arylene ether sulfone) with the same sulfonation degree but without hydroxyl groups (SPES30-HY00) was selected as a reference for characterization. **Table 1** and **Table 2** describe a comparison of several properties of SPES30-HY00 and SPES30-HY30. The hydroxyl groups in a polymer are known to have the ability to form hydrogen bonds with other hydroxyl groups which could result in strengthened physical properties as well as with sulfonic acid groups.³⁸ Therefore, according to the tensile test of two types of membranes, the membrane with hydroxyl group showed improved tensile strength and maximum elongation due to its inter- and intra-molecular hydrogen bond and the higher molecular weight. In addition, as shown in **Table 1**, the 5%

weight loss temperatures of two membranes were approximately 280 °C according to TGA result. This explains that the hydroxyl group does not harm the thermal stability because the decomposition temperature of hydroxyl group was higher than sulfonic groups.³¹

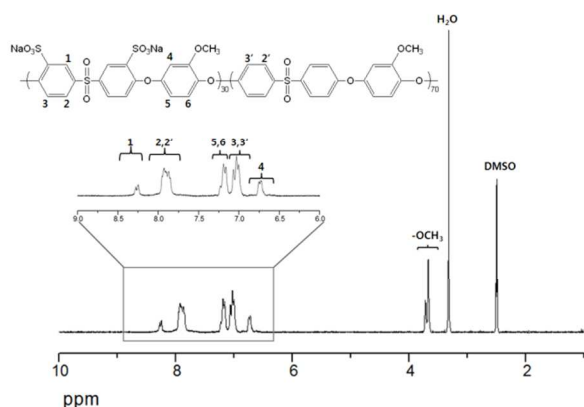


Fig. 2 ¹H NMR spectrum of SPES30-ME100

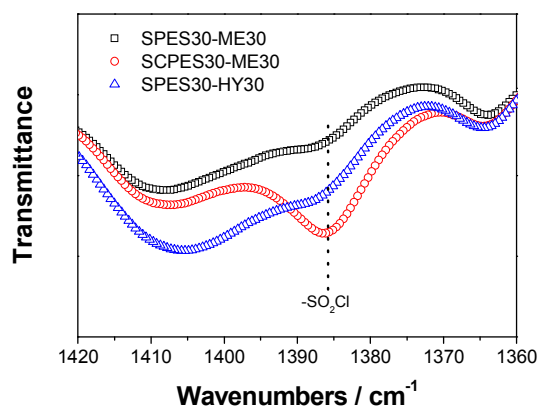


Fig. 3 FT-IR spectra of SPES30-ME30 (–SO₃H, –OCH₃), SCPES30-ME30 (–SO₂Cl, –OCH₃), and SPES30-HY30 (–SO₃H, –OH).

Table 1 Molecular weight and mechanical strength of SPES30-HY00 and SPES30-HY30

	Molecular weight ^a		Mechanical strength ^b		T _{d 5%} (°C)
	M _n	M _w	Tensile strength (MPa)	Elongation at break (%)	
SPES30-HY00	63	175	39	11	278
SPES30-HY30	105	225	50	14	279

^a Determined by GPC using NMP eluent with 0.05 M LiBr.

^b Measured at 18 °C and 45% RH.

The experimental ion exchange capacity (IEC) values that were obtained using a conventional titration test were found to be close to the theoretical values. The water uptake (WU) of a PEM is an important factor that can lead to changes in proton conductivity, dimensional stability, mechanical strength, and

ultimately, membrane electrode assembly (MEA).³⁵ In this experiment, the WU was measured at both low temperature (30 °C) and medium temperature (80 °C). The measured WU of SPES30-HY30 was found to be higher than that of SPES30-HY00; whereas, the IEC values of the two membranes were similar. This was attributed to the –OH group not converting to –O[–]Na⁺ during the ion exchange procedure due to the weak acidity of phenol,³⁹ resulting in an IEC value similar to that of SPES30-HY00. However, the WU results showed that the hydroxyl group worked as a charge carrier, forming a hydrogen-bonded water network in the SPES30-HY30 membrane. The ability of the hydroxyl groups to form hydrogen bonds with water molecules should result in more water being retained within the membrane structure.³⁵ Although WU of membrane increased after hydroxyl side chain was introduced, swelling ratio (SR) results indicates that SPES30-HY30 membrane is stable enough in water at ambient and high temperature.

Table 2 IEC, water uptake and swelling ratio of SPES30-HY00, SPES30-HY30, and SPES40-HY00

	IEC ^a	IEC ^b	Water uptake			
			30 °C		80 °C	
			WU ^c	SR ^d	WU ^c	SR ^d
SPES30-HY00	1.3	1.2	16	15	19	28
SPES30-HY30	1.3	1.2	19	17	29	31

^a Ion exchange capacity (IEC) values calculated by theoretical method (meq./g); ^b IEC values derived by experiments (meq./g); ^c Water uptake (WU (wt%) = (W_{wet} – W_{dry})/W_{dry} × 100); ^d swelling ratio (SR (vol%) = (V_{wet} – V_{dry})/V_{dry} × 100).

Proton conductivity of the polymer electrolytes

Interestingly, we observed highly enhanced proton conductivity values for SPES30-HY30 at operating temperatures of low temperature fuel cell. Fig. 4 shows the proton conductivities of SPES30-HY00 and SPES30-HY30 at 65 °C, 80 °C, and 120 °C at different humidities (30 – 95 %). On varying the temperature and relative humidity, the proton conductivities of SPES30-HY30 ranged from 0.04 to 83 mS cm^{–1}, with the values for SPES30-HY00 being between 0.004 and 16 mS cm^{–1}. Especially, in a low relative humidity condition (30 %), SPES30-HY30 had up to ten times higher proton conductivity than SPES30-HY00, in spite of their similar IEC values. From the proton conductivity result, it is assumed that the hydrogen bonds which were generated between the polymer chains could have an effect on the size and the shape of the hydrophilic nanochannels where proton transport occurs.

As is well known, hydrogen bonding is an essential factor for proton mobility in PEMs.^{40, 41} Protons are transported through the solid membrane via formation and breakage of hydrogen bonds between water molecules and functionalities in the polymer backbone. Nitrile groups have been the most commonly introduced functionalities for producing membranes with better proton conductivities at similar IEC values.^{42–44} In this regard,

hydroxyl groups which are known to have great potential to produce hydrogen bonds were used in the present study in order to create a higher quantity of hydrogen bonds with both water molecules and other hydroxyl groups. By introducing a hydroxyl group to the poly(arylene ether sulfone) membrane, enhanced proton conductivity could be achieved.

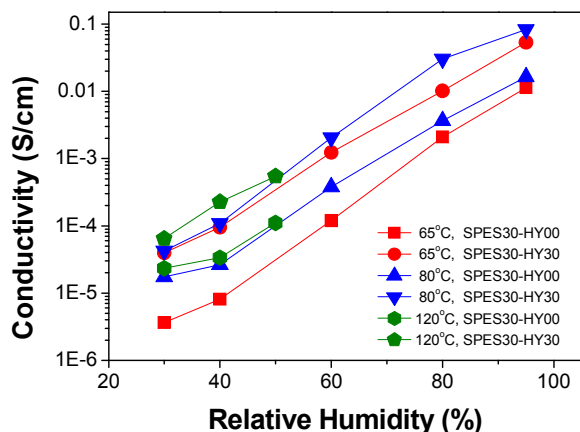


Fig. 4 Proton conductivities of SPES30-HY00 and SPES30-HY30 at various temperatures and relative humidities

Morphological structures of the polymer electrolytes

The evidence which supports the higher proton conductivities of SPES30-HY30 membrane was provided by the microstructure analysis of membranes. In the sulfonated polymer membranes, nanophase separation morphology can be observed between hydrophobic backbone and hydrophilic side chains. The microstructures of SPES30-HY00 and SPES30-HY30 membranes were characterized by using transmission electron microscopy (TEM), as shown in **Fig. 5**. The worm-like phase separated domains were clearly shown in TEM images. The dark regions correspond to the hydrophilic ion channels stained with lead ions, whereas the light regions stand for the hydrophobic polymer matrix.^{32,33} As shown in **Fig. 5**, SPES30-HY30 membrane had larger hydrophilic domains in size and length of 3-5 nm, while SPES30-HY00 membrane had clusters below 2 nm in size. For the TEM image of SPES30-HY30, the interconnected ion clusters were more obvious, which is attributed to the combined effects of both sulfonic acid group and hydroxyl group. The reduced morphological barrier caused by hydroxyl groups, the nano-channels were formed much more effectively for proton transport as observed by TEM. Due to its well-defined phase-separated structure, SPES30-HY30 had the larger number of interconnected hydrophilic domains in the morphology resulting in much higher proton conductivity at low relative humidity.

Single cell performances of the polymer electrolytes

An MEA was fabricated with a catalyst coated membrane (CCM) between two gas diffusion layers (GDLs). The assembled single cell was operated at 65 °C and a relative humidity of 95%. **Fig. 6** presents a comparison of measured polarization and power density curves for SPES30-HY00 and SPES30-HY30. The open circuit voltage (OCV) of SPES30-HY30 (1.00 V) was similar to that of SPES30-HY00 (0.976 V). As the hydroxyl group was introduced to SPES30 membrane, the current density increased from 642 mA cm⁻¹ to 730 mA cm⁻² at the voltage of 0.6 V. In addition, a peak power density also increased from 410 mW cm⁻² to 460 mW cm⁻². The ohmic resistance was calculated from the EIS spectra (**Fig. 7**), and was found to be 0.180 Ω cm² for SPES30-HY30, and 0.223 Ω cm² for SPES30-HY00. Polarization curves were then plotted from these data by excluding the effect of ohmic resistance (Supplementary Figure S1), showing the only effect of membrane type on the performance. The relatively good performance was attributed to high proton conductivity of SPES30-HY30 due to the hydrogen bonds which were produced by inter- and intra-molecular hydroxyl groups. Furthermore, from the linear sweep voltammetry (LSV) test, it was found that the two membranes showed fairly low current densities around 0.4 mA cm⁻² at 0.4 V, indicating that both membranes were durable enough to be applied to single cells due to their low fuel crossovers.

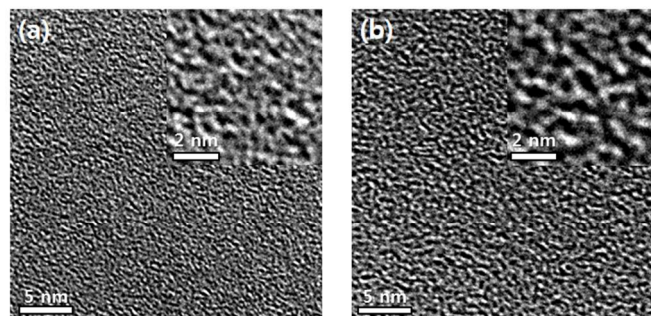


Fig. 5 TEM images of (a) SPES30-HY00 and (b) SPES30-HY30.

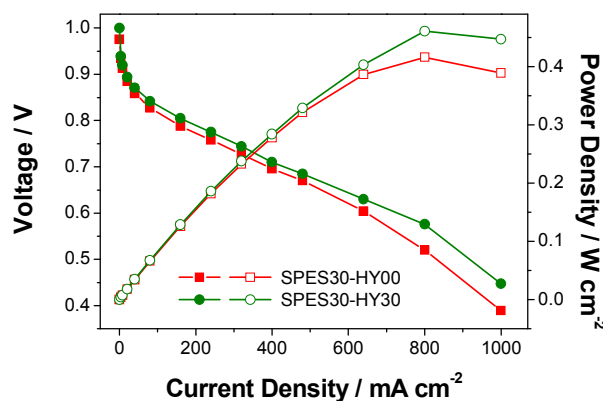


Fig. 6 Polarization curves of SPES30-HY00 (■) and SPES30-HY30 (●) and power density curves of SPES30-HY00 (□) and SPES30-HY30 (○).

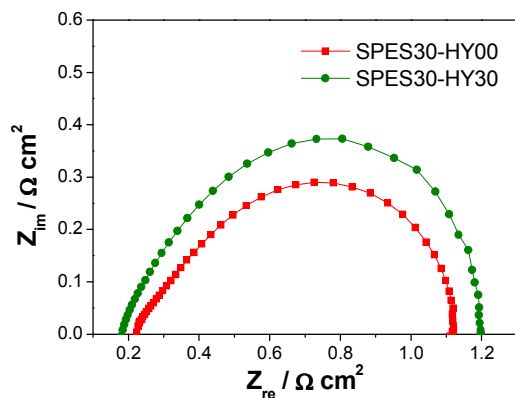


Fig. 7 EIS spectra of two MEAs prepared from SPES30-HY00 and SPES30-HY30.

Conclusions

We have successfully synthesized a new sulfonated poly(arylene ether sulfone) with hydroxyl groups for the first time via four-step reaction. In our synthesized membrane, hydroxyl groups were used to provide additional hydrogen bonding without increasing solubility in water. The newly developed membrane showed excellent properties, in particular regarding proton conductivity resulting in better fuel cell performance without losing its original advantages. The evidence of higher proton conductivity is investigated by the morphology study using TEM and we found that membrane with hydroxyl group had more interconnected hydrophilic clusters than that without hydroxyl group. Although further investigations would be helpful to clarify the optimum ratio of hydroxyl groups for achieving the best and the highest performance, we firmly believe that this type of novel membrane has a great potential to be applicable for fuel cell application.

Experimental

Materials

Bis(4-fluoro-3-sulfohenyl) sulfone disodium salt (SDFDPS) was purchased from Yanjin Technology Co., Ltd. (Tianjin, China). Bis(4-fluorophenyl) sulfone (DFDPS), 2-methoxyhydroquinone, bisphenol A, and potassium carbonate were purchased from Sigma–Aldrich (Seoul, Korea). All other solvents and monomers were obtained from Sigma–Aldrich and used without further purification.

Synthesis of sulfonated poly(arylene ether sulfone)s containing methoxy groups (SPES $_{xx}$ -ME $_{yy}$)

Sulfonated poly(arylene ether sulfone)s with methoxy groups were prepared using a typical copolymerization process utilizing a 250 mL round-bottomed flask, mechanical stirrer, a Dean Stark trap, a condenser, and a gas adapter. The synthetic procedure for the SPES30-ME30 copolymer ($xx = 30$: SDFDPS/DFDPS = 30/70, and $yy = 30$: methoxyhydroquinone/bisphenol A = 30/70) was as follows: A round-bottomed flask was charged with 1.375 g (3 mmol) of SDFDPS, 1.780 g (7 mmol) of DFDPS, 0.420 g (3 mmol) of methoxyhydroquinone, 1.598 g (7 mmol) of bisphenol A, and 2.764 g (20 mmol) of potassium carbonate *N*-methyl-2-pyrrolidone (NMP) was then added to obtain a 10 % solid concentration (w/v), and toluene (typically, NMP/toluene = 2:1 v/v) was introduced after the monomers were completely dissolved in the NMP. The reaction mixture was refluxed at 140 °C for 4 h, and an azeotropic mixture of toluene and water was collected in a Dean Stark trap and then removed over a 60 min time interval. The reaction temperature was slowly increased to 180 °C over 24 h. The resulting viscous solution was diluted with NMP and poured into 1 L of isopropanol and washed several times with deionized water. The obtained copolymer was filtered and dried at 60 °C under vacuum for 24 h.

Conversion of sulfonated groups (SPES $_{xx}$ -ME $_{yy}$) to sulfonyl chloride groups (SCPE $_{Sxx}$ -ME $_{yy}$)

The sulfonated groups of the copolymer were converted into sulfonyl chloride groups using the following procedure: 1.0 g of SPES30-ME30 was dissolved in 20 mL of excess thionyl chloride in a 50 mL one-neck flask equipped with a condenser and an argon inlet. Following this, 1 mL of *N,N*-dimethylformamide (DMF) were added to the solution and reacted at 60 °C for 4 h. During the reaction, hydrogen chloride and sulfur dioxide gas were released, and the reaction was completed simultaneously. The solution was then heated to 95 °C until more than 90 % of the thionyl chloride was distilled off. The remaining solution was cooled to room temperature and diluted by the addition of 10 mL of tetrahydrofuran (THF). The resulting polymeric solution was precipitated in 1 L isopropanol and washed several times with isopropanol until the solution became neutral. Finally, the resulting polymer was filtered and dried at 60 °C under vacuum for 24 h.

Conversion of methoxy groups (SCPE $_{Sxx}$ -ME $_{yy}$) to hydroxyl groups (SPES $_{xx}$ -HY $_{yy}$)

As the sulfonyl chloride groups were formed, SCPE $_{Sxx}$ -ME $_{yy}$ became soluble in dichloromethane (DCM). Demethylation of the methoxy groups in SCPE $_{Sxx}$ -ME $_{yy}$ was then conducted using boron tribromide (1.0 M in DCM). The methoxy groups were transformed into hydroxyl groups through a demethylation process, according to the following steps: 1.0 g of SCPE $_{Sxx}$ -ME $_{yy}$ was dissolved in 30 mL of DCM in a 100 mL two-neck flask with an argon inlet. The reaction bath was cooled to 0 °C and excess 1.0 M boron

tribromide in DCM (7 mL) was injected drop-wise into the reactor. The polymer was rapidly precipitated during this addition, and the reaction mixture was then stirred for a further 6 h. After the reaction, the polymer was filtered directly and washed with boiling water for 24 h. The sulfonyl chloride groups were converted into sulfonic acid groups via hydrolysis in the boiling water conditions. The polymer was then filtered and dried at 60 °C under vacuum for 24 h.

Membrane preparation

The sulfonated polymers with hydroxyl groups were dissolved in NMP to form 2 wt% solutions. Each polymeric solution was then filtered, poured onto a glass plate, and dried under atmospheric pressure at 40 °C for 24 h. The temperature was then gradually increased to 120 °C under vacuum for 48 h. The dried membrane was removed from the glass surface by immersion in a water bath, and the thickness was found to be approximately 40 μm.

Characterization

¹H NMR spectra were recorded on a 300 MHz Bruker AV 300 spectrometer using DMSO-d₆ as the solvent. Fourier transform-infrared (FT-IR) spectra were recorded with a Thermo Mattson Infinity Gold FT-IR 60 AR system. The gel permeation chromatography (GPC) was carried out at 50 °C with Waters 2414 refractive index detector equipped with Styragel HR 3 and 4 columns. NMP was used as an eluent and 0.05 M LiBr was added.

The ion exchange capacities (IEC) of the membranes were measured via a classical titration method using phenolphthalein indicator. After weighing the completely dried membrane, it was immersed in an aqueous solution of 2 M sodium chloride for 48 h at room temperature to release H⁺ ions. The exchanged protons within the solution were then neutralized by addition of a 0.1 N solution of sodium hydroxide, and the IEC values were calculated from the titration results using the following equation:

$$IEC \text{ (mequiv. g}^{-1}\text{)} = \frac{V_{NaOH} \times M_{NaOH}}{W_{dry}}$$

where V_{NaOH} is the added volume of sodium hydroxide, M_{NaOH} is the molarity of sodium hydroxide, and W_{dry} is the weight of the dry membrane sample.

The water uptake (WU) of the membrane was measured by immersing the sample in deionized water for 24 h, and then weighing the wet (W_{wet}) and dry (W_{dry}) membrane. The immersion temperature was set at 30 °C or 80 °C. WU at the two different temperatures was then calculated according to the following equation:

$$WU \text{ (wt\%)} = \frac{W_{wet} - W_{dry}}{W_{dry}} \times 100$$

In addition, the swelling ratio (SR) was calculated from the change in film volume (calculated by multiplying thickness, length, and width) by:

$$SR \text{ (V\%)} = \frac{V_{wet} - V_{dry}}{V_{dry}} \times 100$$

where V_{wet} and V_{dry} are the volumes of the wet and dry membranes.

The mechanical properties of membranes were measured at ambient temperature and relative humidity using a Cometech model QC-508E at a speed of 10 mm/min. The size of the membrane was 1 cm × 4 cm. At least six samples were used for each measurement, and an average value was calculated.

Thermal properties of synthesized polymers were analyzed by thermogravimetric analysis (TGA). Each sample was heated from 10 °C to 1000 °C with a heating rate of 10 °C/min under a nitrogen atmosphere using Universal V4.2E TA Instruments, 2050 TGA.

Proton conductivities of the membranes were measured using AC impedance spectroscopy (IM6 ZAHNER elektrik) with a standard four-probe cell measurement. Each sample was dried and cut into sections 1 × 4 cm in size, and then placed in a temperature and humidity controlled chamber. The IM6 system was used in galvanostatic mode over a frequency range of 100 mHz to 100 kHz. The impedance was measured after the humidity and temperature reached equilibrium. The proton conductivity was calculated using the observed resistance and the following relationship:

$$\text{Proton conductivity } \sigma \text{ (S cm}^{-1}\text{)} = \frac{D}{RA}$$

where D is the distance between the two electrodes, R is the measured resistance, and A is the transverse area of the membrane.

The microstructure of membrane was confirmed by using transmission electron microscopy (TEM) observations. The membrane was stained with lead ions by ion exchange of the sulfonic acid groups and hydroxyl groups in 1.0 M lead acetate aqueous solution. After the lead ions were stained, the membranes were rinsed several times with deionized water, and dried in vacuum oven for 24 h. The membrane was then embedded in epoxy resin and sectioned to 35 nm thickness with ultramicrotome system and placed on copper grids. TEM images were taken with Cryo Tecnai F20 G².

Electrochemical measurement of membrane electrode assembly (MEA)

The MEA was fabricated by inserting a catalyst coated membrane (CCM) between two gas diffusion layers (GDLs). The catalyst slurries were prepared by mixing a platinum/carbon catalyst, water, isopropanol, and 5 wt% Nafion solution with a homogenizer. The catalyst slurries were then

sprayed directly onto the membrane with a platinum loading of 0.4 mg/cm² for both the anode and cathode sides, and the fabricated CCM was dried at 60 °C under vacuum. A single cell was assembled with end plates, graphite bipolar plates, Teflon gaskets, commercial GDLs, and the fabricated CCM. The operating temperature was 65 °C and the relative humidity was 95%. The assembled single cell was activated for 15 h, and the stoichiometric ratios of fuel (hydrogen gas) and oxidant (air) were 1.0 and 3.0, respectively. After activation, current–voltage (I–V), electrochemical impedance spectroscopy (EIS), cyclic voltammetry (CV), and linear sweep voltammetry (LSV) tests were conducted in order to characterize the electrochemical properties of the single cell. EIS was measured by varying the frequency from 50 mHz to 100 kHz. The AC amplitude was 5 mV at an applied potential of 0.85V.

Acknowledgements

This work was supported by the projects “E-Bank” and “COE” from the Korea Institute of Science and Technology.

References

1. T. J. Peckham and S. Holdcroft, *Adv. Mater.*, 2010, **22**, 4667-4690.
2. B. C. H. Steele and A. Heinzl, *Nature*, 2001, **414**.
3. S. Takamuku and P. Jannasch, *Adv. Energy Mater.*, 2012, **2**, 129-140.
4. D. Zhao, J. Li, M.-K. Song, B. Yi, H. Zhang and M. Liu, *Adv. Energy Mater.*, 2011, **1**, 203-211.
5. G. Alberti, M. Casciola, L. Massinelli and B. Bauer, *J. Membr. Sci.*, 2001, **185**, 73-81.
6. S. J. Peighambaroust, S. Rowshanzamir and M. Amjadi, *Int. J. Hydrogen Energy*, 2010, **35**, 9349-9384.
7. B. Smitha, S. Sridhar and A. A. Khan, *J. Membr. Sci.*, 2005, **259**, 10-26.
8. K. Eom, E. Cho, J. Jang, H.-J. Kim, T.-H. Lim, B. K. Hong and J. H. Lee, *Int. J. Hydrogen Energy*, 2013, **38**, 6249-6260.
9. S. Bose, T. Kuila, T. X. H. Nguyen, N. H. Kim, K.-t. Lau and J. H. Lee, *Prog. Polym. Sci.*, 2011, **36**, 813-843.
10. S. Y. Lee, N. R. Kang, D. W. Shin, C. H. Lee, K.-S. Lee, M. D. Guiver, N. Li and Y. M. Lee, *Energy Environ. Sci.*, 2012, **5**, 9795.
11. J. Rozière and D. J. Jones, *Ann. Rev. Mater. Res.*, 2003, **33**, 503-555.
12. J. A. Kerres, *J. Membr. Sci.*, 2001, **185**, 3-27.
13. M. P. Rodgers, L. J. Bonville, H. R. Kunz, D. K. Slattery and J. M. Fenton, *Chem. Rev.*, 2012, **112**, 6075-6103.
14. O. Diat and G. Gebel, *Nature Mater.*, 2008, **7**, 13-14.
15. K. A. Mauritz and R. B. Moore, *Chem. Rev.*, 2004, **104**, 4535-4585.
16. N. Li, S. Y. Lee, Y.-L. Liu, Y. M. Lee and M. D. Guiver, *Energy Environ. Sci.*, 2012, **5**, 5346.
17. F. Wang, M. Hickner, Y. S. Kim, T. A. Zawodzinski and J. E. McGrath, *J. Membr. Sci.*, 2002, **197**, 231-242.
18. K. B. Heo, H. J. Lee, H. J. Kim, B. S. Kim, S. Y. Lee, E. Cho, I. H. Oh, S. A. Hong and T. H. Lim, *J. Power Sources*, 2007, **172**, 215-219.
19. K. B. Wiles, C. M. de Diego, J. de Abajo and J. E. McGrath, *J. Membr. Sci.*, 2007, **294**, 22-29.
20. N. N. Krishnan, D. Henkensmeier, J. H. Jang, H.-J. Kim, H. Y. Ha and S. W. Nam, *Int. J. Hydrogen Energy*, 2013, **38**, 2889-2899.
21. K. T. Park, J. H. Chun, S. G. Kim, B.-H. Chun and S. H. Kim, *Int. J. Hydrogen Energy*, 2011, **36**, 1813-1819.
22. Y.-S. Oh, H.-J. Lee, M. Yoo, H.-J. Kim, J. Han and T.-H. Kim, *J. Membr. Sci.*, 2008, **323**, 309-315.
23. Y. S. Kim, M. A. Hickner, L. Dong, B. S. Pivovar and J. E. McGrath, *J. Membr. Sci.*, 2004, **243**, 317-326.
24. K. D. Kreuer, *J. Membr. Sci.*, 2001, **185**, 29-39.
25. M. A. Hickner, H. Ghassemi, Y. S. Kim, B. R. Einsla and J. E. McGrath, *Chem. Rev.*, 2004, **104**, 4587-4612.
26. F. Wang, M. Hickner, Q. Ji, W. Harrison, J. Mechem, T. A. Zawodzinski and J. E. McGrath, *Macromol. Symp.*, 2001, **175**, 387-395.
27. J. H. Chun, S. G. Kim, J. Y. Lee, D. H. Hyeon, B.-H. Chun, S. H. Kim and K. T. Park, *Renew. Energy*, 2013, **51**, 22-28.
28. G. Alberti and M. Casciola, *Ann. Rev. Mater. Res.*, 2003, **33**, 129-154.
29. K. Yoshimura and K. Iwasaki, *Macromolecules*, 2009, **42**, 9302-9306.
30. D. S. Kim, K. H. Shin, H. B. Park, Y. S. Chung, S. Y. Nam and Y. M. Lee, *J. Membr. Sci.*, 2006, **278**, 428-436.
31. M. Guo, B. Liu, S. Guan, C. Liu, H. Qin and Z. Jiang, *J. Membr. Sci.*, 2010, **362**, 38-46.
32. N. Li, C. Wang, S. Y. Lee, C. H. Park, Y. M. Lee and M. D. Guiver, *Angew. Chem. Int. Edit.*, 2011, **50**, 9158-9161.
33. H. Liao, G. Xiao and D. Yan, *Chem. Commun.*, 2013, **49**, 3979-3981.
34. Y. Lim, D. Seo, M. A. Hossain, S. Lee, J. Lim, H. Jang, T. Hong, Kim and W. Kim, *Electrochim. Acta.*, 2014, **118**, 18-25.
35. C. H. Park, C. H. Lee, M. D. Guiver and Y. M. Lee, *Prog. Polym. Sci.*, 2011, **36**, 1443-1498.
36. J. C. McKeen, Y. S. Yan and M. E. Davis, *Chem. Mater.*, 2008, **20**, 3791-3793.
37. W. Zhang, V. Gogel, K. A. Friedrich and J. Kerres, *J. Power Sources*, 2006, **155**, 3-12.
38. C. Wang, D. W. Shin, S. Y. Lee, N. R. Kang, Y. M. Lee and M. D. Guiver, *J. Membr. Sci.*, 2012, **405-406**, 68-78.
39. R. Morales, *Anal. Chim. Acta.*, 1969, **48**, 309-314.
40. K.-D. Kreuer, S. J. Paddison, E. Spohr and M. Schuster, *Chem. Rev.*, 2004, **104**, 4637-4678.
41. J. K. Clark II and S. J. Paddison, *Electrochim. Acta.*, 2013, **101**, 279-292.
42. M. J. Sumner, W. L. Harrison, R. M. Weyers, Y. S. Kim, J. E. McGrath, J. S. Riffle, A. Brink and M. H. Brink, *J. Membr. Sci.*, 2004, **239**, 199-211.
43. Y. S. Kim, M. J. Sumner, W. L. Harrison, J. S. Riffle, J. E. McGrath and B. S. Pivovar, *J. Electrochem. Soc.*, 2004, **151**, A2150.
44. D. W. Shin, S. Y. Lee, N. R. Kang, K. H. Lee, M. D. Guiver and Y. M. Lee, *Macromolecules*, 2013, **46**, 3452-3460.

Graphical Abstract

